

Accepted Manuscript

Discovery of 1,3-diphenyl-1*H*-pyrazole derivatives containing rhodanine-3-alkanoic acid groups as potential PTP1B inhibitors

Liangpeng Sun, Peipei Wang, Lili Xu, Lixin Gao, Jia Li, Huri Piao

PII: S0960-894X(19)30163-5
DOI: <https://doi.org/10.1016/j.bmcl.2019.03.023>
Reference: BMCL 26337

To appear in: *Bioorganic & Medicinal Chemistry Letters*

Received Date: 16 December 2018
Revised Date: 14 March 2019
Accepted Date: 19 March 2019

Please cite this article as: Sun, L., Wang, P., Xu, L., Gao, L., Li, J., Piao, H., Discovery of 1,3-diphenyl-1*H*-pyrazole derivatives containing rhodanine-3-alkanoic acid groups as potential PTP1B inhibitors, *Bioorganic & Medicinal Chemistry Letters* (2019), doi: <https://doi.org/10.1016/j.bmcl.2019.03.023>

This is a PDF file of an unedited manuscript that has been accepted for publication. As a service to our customers we are providing this early version of the manuscript. The manuscript will undergo copyediting, typesetting, and review of the resulting proof before it is published in its final form. Please note that during the production process errors may be discovered which could affect the content, and all legal disclaimers that apply to the journal pertain.



**Discovery of 1,3-diphenyl-1*H*-pyrazole derivatives containing
rhodanine-3-alkanoic acid groups as potential PTP1B inhibitors**

Liangpeng Sun ^{a, 1}, Peipei Wang ^{b, 1}, Lili Xu ^c, Lixin Gao ^b, Jia Li ^{b,*}, Huri Piao ^{c,*}

^a *College of Medicine, Yanbian University, Yanji, 133000, PR China*

^b *National Center for Drug Screening, Shanghai Institute of Materia Medica, Shanghai Institutes for Biological Science, Chinese Academy of Sciences, Shanghai 201203, China*

^c *Key Laboratory of Natural Resources of Changbai Mountain & Functional Molecules, Ministry of Education, Yanbian University College of Pharmacy, Yanji, 133000, PR China*

* Corresponding author. Tel: + 86 433 2436149

E-mail address: piaohr@ybu.edu.cn (H. -R. Piao)

* Co-corresponding author. Tel/Fax: + 86 21 50800721

E-mail address: jli@simm.ac.cn (J. Li)

¹ These authors contributed equally to this work.

Abstract

Two series of 1,3-diphenyl-1*H*-pyrazole derivatives containing rhodanine-3-alkanoic acid groups were identified as competitive protein tyrosine phosphatase 1B (PTP1B) inhibitors. Among the compounds studied, **IIIv** was found to have the best *in vitro* inhibition activity against PTP1B ($IC_{50} = 0.67 \pm 0.09 \mu\text{M}$) and the best selectivity (9-fold) between PTP1B and T-cell protein tyrosine phosphatase (TCPTP). Molecular docking studies demonstrated that compounds **III**m, **III**v and **IV**g could occupy simultaneously at both the catalytic site and the adjacent pTyr binding site. These results provide novel lead compounds for the design of inhibitors of PTP1B as well as other PTPs.

Keywords: PTP1B inhibitor; 1,3-Diphenyl-1*H*-pyrazole; Rhodanine-3-alkanoic acid

Protein tyrosine phosphatases (PTPs) play an important regulatory role in the intracellular phosphorylation state of proteins.¹ Unregulated PTP activity is responsible for several human diseases including cancer, diabetes, obesity and dysfunction of the immune system.²⁻⁴ Among the PTPs, protein tyrosine phosphatase 1B (PTP1B) activates c-Src in human breast cancer and also downregulates insulin signaling by dephosphorylating the insulin receptor (IR), insulin receptor substrate-1 (IRS-1) and insulin receptor substrate-2 (IRS-2).⁵⁻⁶ Additionally, PTP1B is a negative regulator in the leptin signaling pathway and dephosphorylates JAK2, a kinase downstream of the leptin receptor.⁷⁻⁸ PTP1B knockout mice exhibit phenotypes of increased insulin sensitivity, improved glucose tolerance and resistance to diet-induced obesity.⁹⁻¹⁰ Therefore, PTP1B could be a useful target for the treatment of type 2 diabetes mellitus, obesity and cancer, and small molecule inhibitors of PTP1B may be promising drug candidates for treating these diseases.

In recent years, following the elucidation of the basic structural requirements for PTP1B-substrate and -inhibitor interactions, a large variety of potent PTP1B inhibitors have been identified through high-throughput screening, structure-based and fragment-based drug design. The low cell permeability and bioavailability of

these compounds have limited their development as effective drugs because of the presence of highly negatively charged residues (including difluoromethylphosphonates, carboxymethylsalicylic acids and oxalylaminobenzoic acids) that mimic the phosphate group in IRS.¹¹⁻¹² Additionally, because of the structural homology present throughout many PTP families, it is challenging to identify selective inhibitors specific to each PTP. Hence, it is imperative to identify novel compounds with new core scaffolds that inhibit PTP1B with sufficient efficacy and desirable pharmaceutical properties.

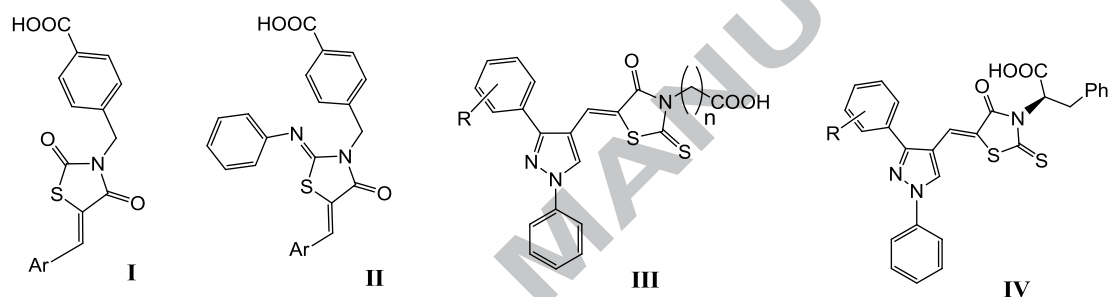


Figure 1. Structures of known PTP1B inhibitors (**I** and **II**) and rhodanine-3-alkanoic acid derivatives (**III** and **IV**).

Because of the electrostatic properties of the PTP1B enzyme active site,¹³ it has proven difficult to develop effective uncharged pTyr mimetics. Replacing the phosphate group of pTyr with bioisosteric monoanionic groups, such as carboxylates, is considered a valid method to obtain inhibitors with low polarity.¹⁴⁻¹⁵ Indeed, several carboxylic acids with good PTP1B inhibitory profiles and cellular activity or oral bioavailability have been reported.¹⁶⁻²² For example, as shown in Figure 1, compound **I** was identified as inhibitors of PTP1B, in which a 4-[(2,4-dioxothiazolidin-3-yl)methyl]benzoic acid moiety could act as a monoanionic pTyr-mimetic group and replicate the interactions of pTyr with the catalytic site of the enzyme and the 5-arylidene moiety could bind the surrounding lipophilic amino acid residues, including the PTP1B secondary noncatalytic binding pocket.²¹ Subsequent studies showed that compound **II**, where a 2-phenylimino moiety was introduced into the 4-thiazolidinone ring, could further enhance the affinity between the inhibitor and

enzyme by means of favorable interactions with active site residues and the surrounding loops.²² Moreover, these compounds were capable to induce the insulin metabolic pathway in mouse C2C12 skeletal muscle cells by remarkably stimulating both IR β phosphorylation and 2-deoxyglucose cellular uptake.¹⁸

In our previous work, a large variety of rhodanine-3-alkanoic acid derivatives (e.g. **III** and **IV**) were synthesized and identified as potential antibacterial agents.²³⁻²⁶ The structures of 4-[(2, 4-dioxothiazolidin-3-yl)methyl]benzoic acid (**V**) and rhodanine-3-acetic acid (**VII**) are based on similar scaffolds. According to the strategy of pharmacophore-oriented scaffold hopping, we assumed by extension that rhodanine-3-acetic acid derivatives might possess inhibition activity against PTP1B. Inspired by the fragment **VI**, we assumed that a (*R*)-2-(4-oxo-2-thioxothiazolidin-3-yl)-3-phenylpropanoic acid group (**VIII**) might offer a possible alternative skeleton which could bind simultaneously in both the catalytic site and the adjacent pTyr binding site, and improve not only the binding affinity but also the opportunity for selectivity over other PTPs (Figure 2).

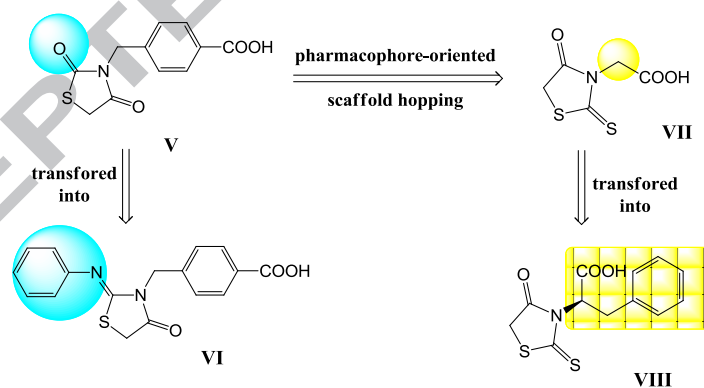
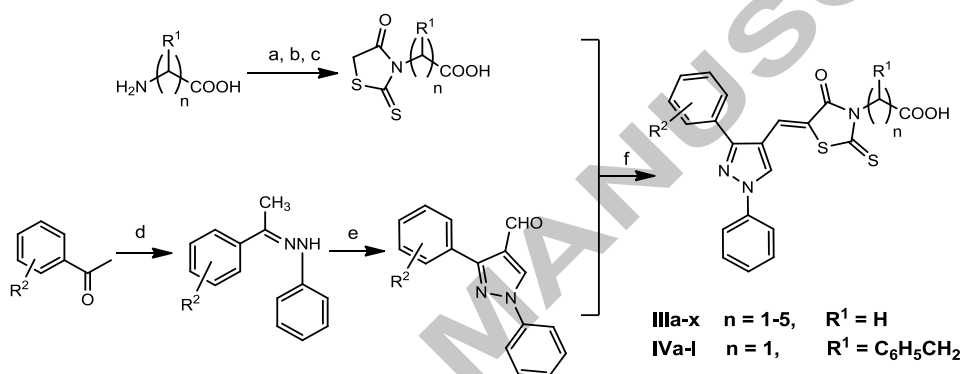


Figure 2. Design strategies of the novel pTyr mimetic based pharmacophore-oriented scaffold hopping.

To expand the range of available pharmacophores from which new PTP1B inhibitors can be developed, compounds **III** and **IV** were selected and tested against PTP1B. Interestingly, most of the tested compounds showed good PTP1B inhibitory activity at 20 $\mu\text{g/mL}$ and dose-dependently inhibited PTP1B with IC_{50} values in the micromolar range as expected. In the present work, we report a class of rhodanine

compounds as novel and potent inhibitors of PTP1B. Additionally, the mechanism of inhibition of PTP1B by these compounds along with their structure–activity relationships (SARs) were probed, which provides insights for further optimization of lead compounds of this class and generation of a pharmacophore model.

Compounds **III** and **IV** were synthesized according to Scheme 1. The synthetic procedures to generate compounds **III** and **IV** along with their spectral data were previously described by our laboratory.²⁵⁻²⁶



Scheme 1. Regants and conditions: (a) carbon disulfide, NaOH, 25 °C, 16 h; (b) sodium chloroacetate, 25 °C, 3 h; (c) 6M HCl, reflux, 16 h. (d) phenylhydrazine, acetic acid, NaOH, CH₃CH₂OH, reflux, 1h; (e) (i) *N,N*-dimethylformamide, POCl₃, 0-5 °C, 0.5 h; (ii) *N,N*-dimethylformamide, 50 °C; (f) piperidine, acetic acid, CH₃CH₂OH, 40-50 °C, 4 h.

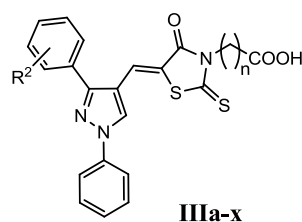
The inhibitory activities of all the compounds against PTP1B were measured using *p*-nitrophenyl phosphate (*p*NPP) as a substrate, and the results are summarized in Tables 1 and 2. The known PTP1B inhibitor oleanolic acid (IC₅₀ = 1.62 ± 0.13 μM) was used as the positive control.^{17, 27} As shown in Tables 1 and 2, 27 out of 36 compounds tested showed good PTP1B inhibitory activity at 20 μg/mL and dose-dependently inhibited PTP1B with IC₅₀ values ranging from 0.67 ± 0.09 to 24.56 ± 1.21 μM. Of these, **IIIv** was the most potent with an IC₅₀ value of 0.67 ± 0.09 μM, about 2.5-fold better than that of the positive control.

The following SARs were obtained by analyzing the activities of compounds **III** and **IV**. As shown in Table 1, among compounds **IIIa-p** containing rhodanine-3-acetic acid, seven compounds (e.g. **III d**, **III g**, **III h**, **III i**, **III k**, **III m** and **III n**) exhibited inhibitory activities against PTP1B (IC₅₀ = 4.78 ± 0.27 ~ 24.56 ± 1.21

μM). These results indicated that the PTP1B inhibitory activity was significantly influenced by the position and nature of the substituent on the phenyl ring. The impact of the substituent position on the benzene ring on the efficacy was not predictable. Compared with compounds **IIIj** and **IIIm**, the compound with the phenyl ring substituent (**IIIj**) showed no activity at $20 \mu\text{g/mL}$, but interestingly, the compound with the naphthalene ring (**IIIm**) had dramatically improved PTP1B inhibitory activity with an IC_{50} value of $4.78 \pm 0.27 \mu\text{M}$. This is consistent with earlier studies in which lipophilic moieties stabilized the enzyme–compound complex via hydrophobic interactions with the active site and surrounding subpockets, a common feature of PTP1B–inhibitor complexes.¹⁸⁻²² This concept is also supported by our docking simulations as described below (Figure 5B). To investigate the effects of the substituents on the nitrogen atom of the rhodanine on the PTP1B inhibitory activity, the acetic acid moiety was changed to various fatty acids with different carbon chain lengths while simultaneously fixing the substituents on the phenyl ring, such as 2, 4-chlorine or 4-chlorine. Interestingly, the results for the 2-thioxo-4-thiazolidinone N-alkanoic acids derivatives (**IIIq–x**) showed that increasing the length of the carbon chain resulted in a significant increase of inhibitory activity, in particular, compound **IIIv** was found to have the best inhibitory activity against PTP1B ($\text{IC}_{50} = 0.67 \pm 0.09 \mu\text{M}$). This result suggests that the carbon chain length between the COOH group and 2-thioxo-4-thiazolidinone ring plays a crucial role in determining the inhibitor binding affinity. In this regard, more derivatives possessing different rhodanine-3-fatty acids need to be designed and synthesized to establish the optimum length required for the best inhibitory potency, and this work is currently in progress in our laboratory.

Table 1

Inhibitory activity of compounds **IIIa–x** against PTP1B.



Compound	R ²	n	IC ₅₀ (μM) ^a	Compound	R ²	n	IC ₅₀ (μM)
IIIa	2-F	1	NA ^b	IIIm	Phenyl (3,4-fused)	1	4.78 ± 0.27
IIIb	4-F	1	NA	IIIn	2-OCH ₃	1	24.56 ± 1.21
IIIc	2-Cl	1	NA	IIIo	3-OCH ₃	1	NA
IIIc	2-Cl	1	NA	IIIp	4-OCH ₃	1	NA
IIIe	4-Cl	1	NA	IIIq	4-Cl	2	6.58 ± 1.76
IIIe	4-Cl	1	NA	IIIr	2,4-Cl ₂	2	7.93 ± 0.42
IIIe	4-Cl	1	NA	IIIr	2,4-Cl ₂	2	7.93 ± 0.42
IIIf	2,4-Cl ₂	1	NA	IIIr	2,4-Cl ₂	2	7.93 ± 0.42
IIIg	3-Br	1	12.14 ± 1.64	IIIr	2,4-Cl ₂	2	7.93 ± 0.42
IIIg	3-Br	1	12.14 ± 1.64	IIIr	2,4-Cl ₂	2	7.93 ± 0.42
IIIg	3-Br	1	12.14 ± 1.64	IIIr	2,4-Cl ₂	2	7.93 ± 0.42
IIIh	4-Br	1	14.22 ± 0.30	IIIr	2,4-Cl ₂	2	7.93 ± 0.42
IIIh	4-Br	1	14.22 ± 0.30	IIIr	2,4-Cl ₂	2	7.93 ± 0.42
IIIh	4-Br	1	14.22 ± 0.30	IIIr	2,4-Cl ₂	2	7.93 ± 0.42
IIIi	4-NO ₂	1	9.24 ± 0.60	IIIr	2,4-Cl ₂	2	7.93 ± 0.42
IIIi	4-NO ₂	1	9.24 ± 0.60	IIIr	2,4-Cl ₂	2	7.93 ± 0.42
IIIi	4-NO ₂	1	9.24 ± 0.60	IIIr	2,4-Cl ₂	2	7.93 ± 0.42
IIIj	H	1	NA	IIIr	2,4-Cl ₂	2	7.93 ± 0.42
IIIj	H	1	NA	IIIr	2,4-Cl ₂	2	7.93 ± 0.42
IIIj	H	1	NA	IIIr	2,4-Cl ₂	2	7.93 ± 0.42
IIIk	4-CH ₃	1	14.68 ± 3.08	IIIr	2,4-Cl ₂	2	7.93 ± 0.42
IIIk	4-CH ₃	1	14.68 ± 3.08	IIIr	2,4-Cl ₂	2	7.93 ± 0.42
IIIk	4-CH ₃	1	14.68 ± 3.08	IIIr	2,4-Cl ₂	2	7.93 ± 0.42
III	2,4-(CH ₃) ₂	1	NA	IIIr	2,4-Cl ₂	2	7.93 ± 0.42
III	2,4-(CH ₃) ₂	1	NA	IIIr	2,4-Cl ₂	2	7.93 ± 0.42
III	2,4-(CH ₃) ₂	1	NA	IIIr	2,4-Cl ₂	2	7.93 ± 0.42
Oleanolic acid ^c			1.62 ± 0.13	IIIr	2,4-Cl ₂	2	7.93 ± 0.42

^a The pNPP assay. IC₅₀ values were determined by regression analyses and expressed as means ± SD of three replications.

^b Not active at 20 μg/mL concentration.

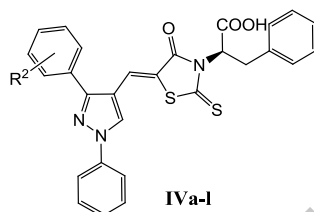
^c Positive control.

As shown in Table 2, phenylalanine-derived rhodanine derivatives (**IVa-l**) generally exhibited higher levels of inhibitory activity compared with the corresponding rhodanine-3-acetic acid compounds (**IIIc**, **IIIe-k** and **IIIm-p**). As expected, introducing a benzyl group at the 2-position of the carboxyl group remarkably affected the activity, which might be attributed to the ability of the phenyl ring to form steric interactions with Phe182, Met258, Leu260 and Gln262 as suggested by the docking study (Figure 5D). On the basis of these observations, we inferred that introduction of different substituents at the 2-position of the carboxyl group might influence the PTP1B inhibitory activity. Thus it was necessary to make further structural modifications at the 2-position to optimize the binding potency in the tyrosine phosphate binding pocket of the active site. The compounds with electron-withdrawing groups on the phenyl ring (**IVa-f**) showed better activity than compounds **IVi-l** containing electron-donating groups. These results indicated that electron-withdrawing groups contributed more to the inhibitory activity of PTP1B than electron-donating groups. Interestingly, compound **IVg** containing the

naphthalene group ($IC_{50} = 1.81 \pm 0.22 \mu\text{M}$) dramatically improved the enzyme inhibitory activity as **IVg** was 3.5-fold more potent than compound **IVh** ($IC_{50} = 6.37 \pm 0.52 \mu\text{M}$). A similar trend was also observed for compounds identified as part of the **III** numerical series.

Table 2

Inhibitory activity of compounds **IVa-l** against PTP1B.



Compound	R ²	IC ₅₀ (μM) ^a	Compound	R ²	IC ₅₀ (μM)
IVa	2-Cl	4.89 ± 0.47	IVg	Phenyl (3,4-fused)	1.81 ± 0.22
IVb	4-Cl	2.10 ± 0.34	IVh	H	6.37 ± 0.52
IVc	2,4-Cl ₂	3.56 ± 0.20	IVi	4-CH ₃	2.05 ± 0.21
IVd	3-Br	2.76 ± 0.55	IVj	2-OCH ₃	6.30 ± 1.46
IVe	4-Br	4.42 ± 0.91	IVk	3-OCH ₃	4.95 ± 0.42
IVf	4-NO ₂	3.57 ± 0.41	IVl	4-OCH ₃	7.09 ± 0.81
Oleanolic acid ^b		1.62 ± 0.13			

^a The pNPP assay. IC₅₀ values were determined by regression analyses and expressed as means ± SD of three replications.

^b Positive control.

A number of representative compounds (e.g. **III**m, **III**r, **III**t, **III**v, **III**x, **IV**c and **IV**g) were investigated for their selectivity toward other PTPs by the same method,¹⁷ including TCPTP, cell division cycle 25 homolog B (CDC25B), leukocyte antigen-related phosphatase (LAR), src homology phosphatase-1 (SHP-1) and src homology phosphatase-2 (SHP-2). As shown in Table 3, these compounds showed 2- to 9-fold greater selectivity for PTP1B than for TCPTP. None of the compounds inhibited LAR activity at 20 μg/mL. We concluded that these compounds possessed about 3- to 42-fold selectivity for PTP1B over CDC25B. The compounds had no visible activities toward SHP-1 and SHP-2 (except for **III**m and **IV**c).

Table 3

Inhibitory activity of selected compounds against related PTPs.

Compound	IC ₅₀ ^a (μM)					
	PTP1B	TCPTP	CDC25B	LAR	SHP-1	SHP-2
III_m	4.78 ± 0.27	7.91 ± 0.93	11.30 ± 0.65	NA ^b	24.45 ± 1.10	20.91 ± 1.42
III_r	7.93 ± 0.42	14.05 ± 1.64	17.10 ± 1.01	NA	NA	NA
III_t	3.66 ± 0.38	9.18 ± 1.35	13.81 ± 0.32	NA	NA	NA
III_v	0.67 ± 0.09	5.77 ± 0.35	28.15 ± 3.00	NA	NA	NA
III_x	1.35 ± 0.27	5.63 ± 0.47	10.90 ± 0.49	NA	NA	NA
IV_c	3.56 ± 0.20	12.66 ± 1.67	13.72 ± 2.92	NA	16.81 ± 1.01	16.67 ± 1.06
IV_g	1.81 ± 0.22	4.61 ± 0.42	6.12 ± 0.92	NA	NA	NA
Na ₃ VO ₄ ^c	— ^d	—	2.08 ± 0.16	15.14 ± 0.23	26.14 ± 1.65	24.05 ± 0.95
Oleanolic acid ^c	1.62 ± 0.13	4.89 ± 0.63	—	—	—	—

^a The *p*NPP assay. IC₅₀ values were determined by regression analyses and expressed as means ± SD of three replications.

^b Not active at 20 μg/mL concentration.

^c Positive control.

^d Not tested.

A kinetic study was performed to investigate the inhibitory mechanism of compounds **III_v** and **IV_g**.²⁷ As shown in Figure 3A and 4A, **III_v** and **IV_g** demonstrated a time-independent inhibition of PTP1B, which showed **III_v** and **IV_g** were fast-binding inhibitors of PTP1B. The time-independent inhibition of **III_v** and **IV_g** towards PTP1B may also exclude that **III_v** and **IV_g** were nonspecific inhibitors, because nonspecific inhibitors always show time-dependent behavior and steep inhibition curve.²⁸ As shown in Figure 3B and 4B, the inhibition modality of **III_v** and **IV_g** toward PTP1B exhibited characteristics typical of a competitive inhibitor, including increased K_m values and unchanged V_{max} values following increases in inhibitor concentration. The Lineweaver-Burk plot also indicated that **III_v** and **IV_g** were competitive inhibitors of PTP1B as shown by the intersection of the best fit lines on the y-axis (Figure 3C and 4C). These results indicate that **III_v** and **IV_g** bind to the catalytic pocket of PTP1B and behave as competitors to the physiological substrate. The K_i values were calculated as 0.31 μM and 0.70 μM, respectively.

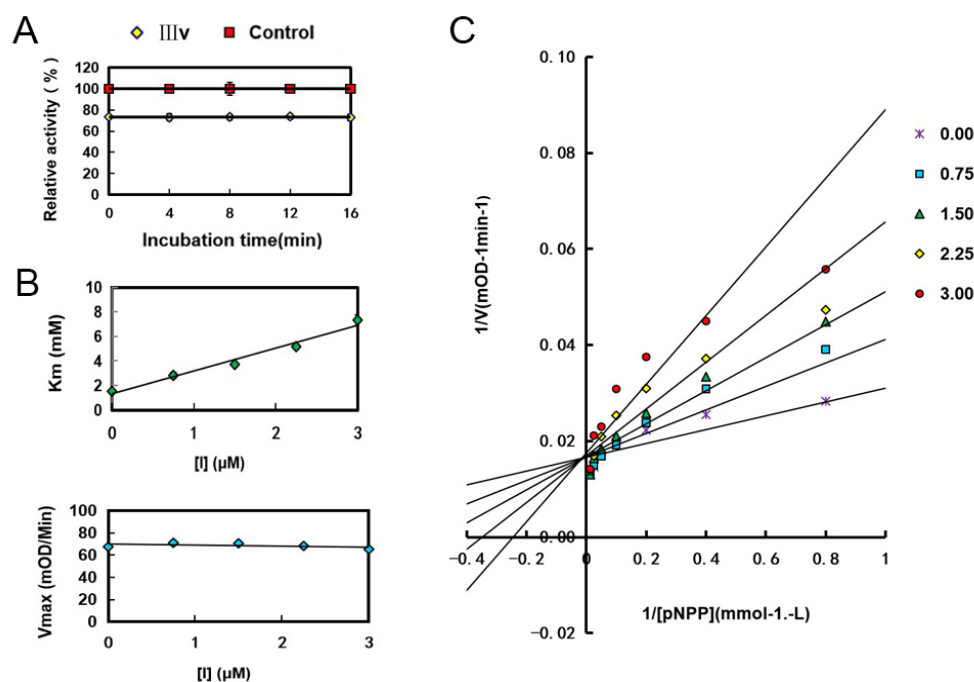


Figure 3. Characterization of **IIIv** to PTP1B.

(A) Time-independent inhibition of PTP1B by **IIIv**. (B) At various fixed concentrations of **IIIv** the initial velocity was determined with various concentrations of *p*NPP. (C) Typical competitive inhibition of **IIIv** shown by Lineweaver-Burk plot.

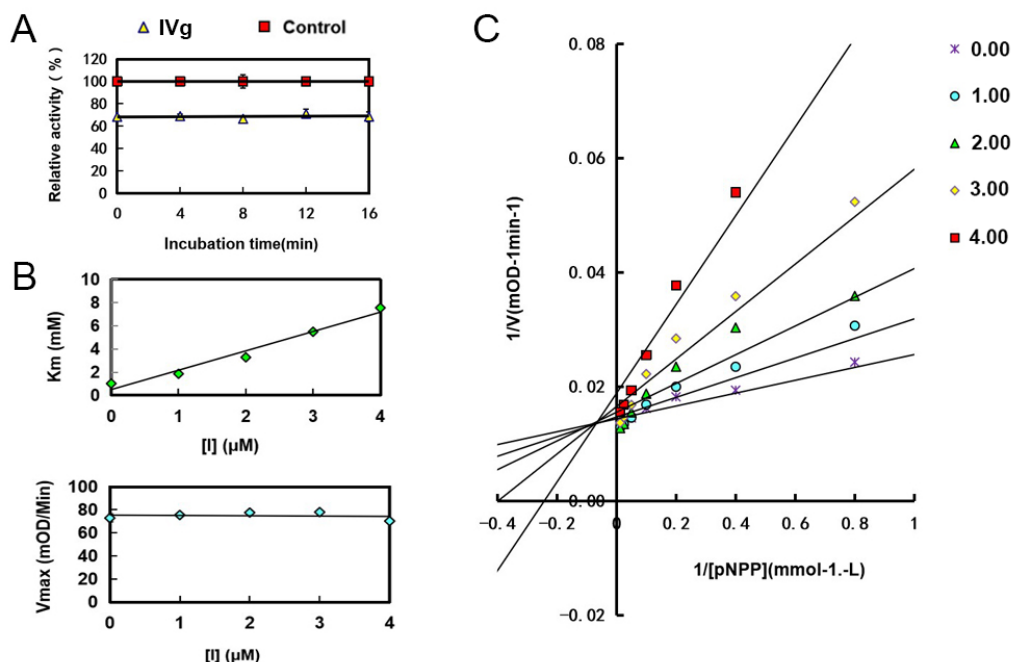


Figure 4. Characterization of **IVg** to PTP1B.

(A) Time-independent inhibition of PTP1B by **IVg**. (B) At various fixed concentrations of **IVg** the initial velocity was determined with various concentrations of *p*NPP. (C) Typical competitive inhibition of **IVg** shown by Lineweaver-Burk plot.

To understand the inhibitory activities of **III**m, **III**v and **IV**g against PTP1B, we subjected them to molecular docking analysis using MOE Dock in MOE v2014.0901²⁹ and predicted their binding affinity with PTP1B (PDB code: 2vey).³⁰ The binding modes of three compounds revealed by docking studies are illustrated in Figure 5. These results indicated that their interaction modes were similar to those of compounds **I** and **II**,²¹⁻²² in which the rhodanine-3-alkanoic acid moieties were situated in the catalytic site of PTP1B and the 1,3-diaryl pyrazole group extended into the hydrophobic subpocket near the catalytic site.

As shown in Figure 5B, the carbonyl and hydroxyl moieties of the carboxyl group in **III**m, regarded as the hydrogen bond acceptor and donor, respectively, form hydrogen bonds with the backbone of Gly220 and side chain of Cys215 in the catalytic site of PTP1B, respectively. The naphthalene ring showed good van der Waals interactions with Met258, Gln262 and Asp48 in PTP1B, indicating it might contribute to the improved activities of this compound compared with **III**j. Additionally, the terminal benzene ring provided good van der Waals interactions with Tyr46 and Phe182 in PTP1B.

As shown in Figure 5D, the oxygen atom of the carboxyl group in **IV**g, regarded as the hydrogen bond donor, forms one hydrogen bond with the sidechain of Cys215 in PTP1B. The sulfur atom of the carbon-sulfur double bond of the thiazole ring, regarded as the hydrogen bond acceptor, forms one hydrogen bond with the sidechain of Phe182 in PTP1B. Some van der Waals interactions were also observed, including interactions of the naphthalene ring with Asp48, Arg47 and Met258 and interactions of the terminal benzene ring with Tyr46 and Arg45. The benzyl group of the adjacent carboxyl group provides good van der Waals interactions with Phe182, Met258, Leu260 and Gln262 in PTP1B, which might explain the activity difference between compounds **IV** and **III**a–p.

As shown in Figure 5F, the pyrazole of **III**v forms a H- π conjugation with the sidechain of Gln262 in PTP1B. The sulfur atom of the thiazole and carbon atom of the adjacent vinyl moiety, regarded as a hydrogen bond acceptor, forms two hydrogen bonds with the sidechain of Asp48 in PTP1B. The carbonyl and hydroxyl moieties of

the carboxyl group, regarded as the hydrogen bond acceptor and donor, forms three hydrogen bonds with the backbone of Ser216 and sidechains of Arg221 and Cys215 in PTP1B. Some van der Waals interactions were also observed, such as interactions between the terminal benzene ring and Gly259 and Arg24, the sulfur atom of the carbon-sulfur double bond of the thiazole ring and Met258, and the sulfur atom of the thiazole ring and Asp48.

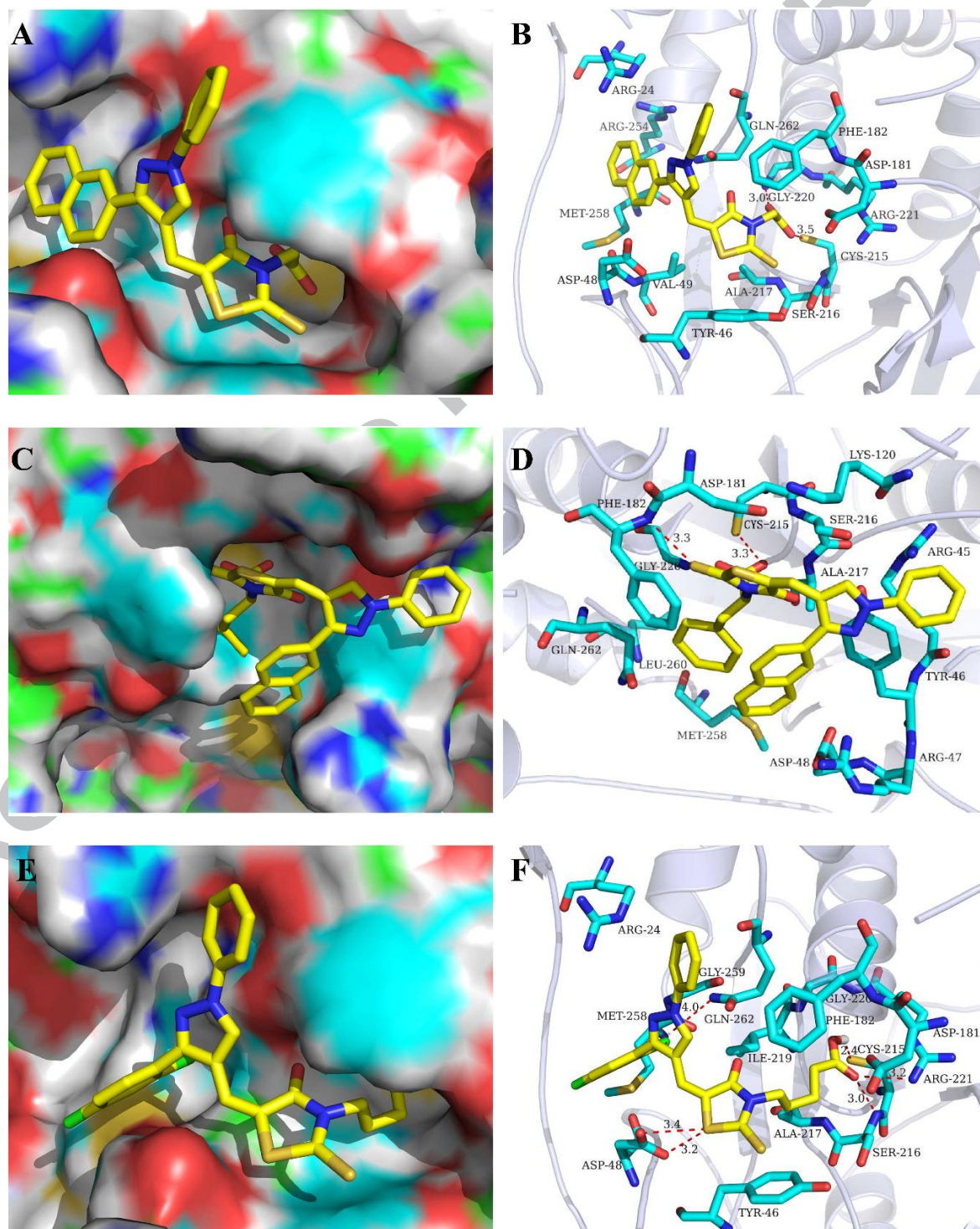


Figure 5. The binding model of **III_m**, **III_v** and **IV_g** with PTP1B. (A) The binding model of **III_m** on molecular surface of PTP1B. (B) The interaction model of **III_m** with PTP1B. (C) The binding model of **IV_g** on molecular surface of PTP1B. (D) The interaction model of **IV_g** with PTP1B. (E) The binding model of **III_v** on molecular surface of PTP1B. (F) The interaction model of **III_v** with PTP1B. The ligands are colored in yellow, and the surrounding residues in the binding pockets are colored in cyan. The backbone of the receptor is depicted as light blue ribbon.

The Asp48 residue provided the specificity of PTP1B for phosphotyrosine over phosphoserine or phosphothreonine and the Gly220 residue of PTP1B was important in modulating the activities according to previous studies.³¹ Taken together, the docking simulation studies indicate that **III_m** interacts with Gly220 and Cys215 of PTP1B through hydrogen bonds, **IV_g** interacts with Cys215 and Phe182 of PTP1B through hydrogen bonds, and **III_v** interacts with Asp48, Gln262, Ser216, Arg221 and Cys215 of PTP1B through hydrogen bonds and H- π conjugation. The different binding models between ligands and PTP1B result in different binding abilities. The docking scores of **III_m**, **III_v** and **IV_g** are shown in Table 4, which are -7.3611 kcal/mol, -8.2432 kcal/mol and -7.3841 kcal/mol for PTP1B, respectively. The computational results indicate that **III_m**, **III_v** and **IV_g** all interact with PTP1B and the binding ability with PTP1B is in the order **III_v** > **IV_g** > **III_m**.

Table 4

The docking score of molecules binding with PTP1B.

Ligands	Receptor	Docking score (kcal/mol)
III_m	PTP1B	-7.3611
III_v	PTP1B	-8.2432
IV_g	PTP1B	-7.3841

In summary, two series of 1,3-diaryl pyrazole derivatives containing rhodanine-3-alkanoic acid groups were identified as novel competitive PTP1B inhibitors with IC₅₀ values in the micromolar range. Compound **III_v** showed the best PTP1B inhibitory potency (IC₅₀ = 0.67 ± 0.09 μ M) and the best selectivity (9-fold) between PTP1B and TCPTP. This preliminary SAR study highlighted that the carbon chain length of the alkanolic acid and introduction of a benzyl group at the 2-position

of the carboxyl group remarkably improved the PTP1B inhibitory activity and selectivity toward other PTPs. Molecular docking studies of three compounds (**III**m, **III**v and **IV**g) indicated that the rhodanine-3-alkanoic acid moieties were situated in the catalytic site of PTP1B and the 1,3-diaryl pyrazole group extended into the hydrophobic subpocket near the catalytic site, which indicated a possible binding mode and provided insights for further optimization of the scaffold. The design and synthesis of new potential PTP1B inhibitors based on the available biological data and SAR analysis are currently ongoing in our research group.

Acknowledgments

We wish to thank the National Natural Science Foundation of China (No. 81460524 and 81773779) and the Education Department of Jilin Province Scientific Research Fund Project (2015-50) for financial support. We thank Renee Mosi, PhD, from Liwen Bianji, Edanz Group China (www.liwenbianji.cn/ac), for editing the English text of a draft of this manuscript.

References and notes

1. Tonks, N. K. *Cell* **2005**, *121*, 667.
2. Zhang, Z. Y. *Curr. Opin. Chem. Biol.* **2001**, *5*, 416.
3. Zhang, Z. Y. *Biochimica Biophysica Acta.* **2005**, *1754*, 100.
4. Julien, S. G.; Dubé, N.; Hardy, S.; Tremblay, M. L. *Nat. Rev. Cancer* **2011**, *11*, 35.
5. Goldstein, B. J.; Bittner-Kowalczyk, A.; Harbeck, M. *J. Biol. Chem.* **2000**, *275*, 4283.
6. Wälchli, S.; Curchod, M. L.; HooftvanHuijsdijnen, R. *J. Biol. Chem.* **2000**, *275*, 9792.
7. Cheng, A.; Uetani, N.; Simoncic, P. D.; Tremblay, M. L. *Dev. Cell* **2002**, *2*, 497.

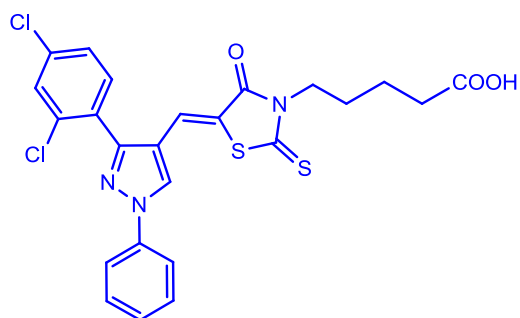
8. Cook, W. S.; Unger, R. H. *Dev. Cell* **2002**, *2*, 385.
9. Elchebly, M.; Payette, P.; Michaliszyn, E.; Cromlish, W.; Collins, S.; Loy, A. L.; Normandin, D.; Cheng, A.; Himms-Hagen, J.; Chan, C. C.; Ramachandran, C.; Gresser, M. J.; Tremblay, M. L.; Kennedy, B. P. *Science* **1999**, *283*, 1544.
10. Klamn, L. D.; Boss, O.; Peroni, O. D.; Kim, J. K.; Martino, J. L.; Zabolotny, J. M.; Moghal, N.; Lubkin, M.; Kim, Y. B.; Sharpe, A. H.; Stricker-Krongrad, A.; Shulman, G. I.; Neel, B. G.; Kahn, B. B. *Mol. Cell Biol.* **2000**, *20*, 5479.
11. Combs, A. P. *J. Med. Chem.* **2010**, *53*, 2333.
12. Tamrakar, A. K.; Maurya, C. K.; Rai, A. K. *Expert Opin. Ther. Pat.* **2014**, *24*, 1101.
13. Sarmiento, M.; Puius, Y. A.; Vetter, S. W.; Keng, Y. F.; Wu, L.; Zhao, Y.; Lawrence, D. S.; Almo, S. C.; Zhang, Z. Y. *Biochemistry* **2000**, *39*, 8171.
14. Xin, Z.; Liu, G.; Abad-Zapatero, C.; Pei, Z.; Szczepankiewicz, B. G.; Li, X.; Zhang, T.; Hutchins, C. W.; Hajduk, P. J.; Ballaron, S. J.; Stashko, M. A.; Lubben, T. H.; Trevillyan, J. M.; Jirousek, M. R. *Bioorg. Med. Chem. Lett.* **2003**, *13*, 3947.
15. Zhao, H.; Liu, G.; Xin, Z.; Serby, M. D.; Pei, Z.; Szczepankiewicz, B. G.; Hajduk, P. J.; Abad-Zapatero, C.; Hutchins, C. W.; Lubben, T. H.; Ballaron, S. J.; Haasch, D. L.; Kaszubska, W.; Rondinone, C. M.; Trevillyan, J. M.; Jirousek, M. R. *Bioorg. Med. Chem. Lett.* **2004**, *14*, 5543.
16. Zhang, W.; Hong, D.; Zhou, Y.; Zhang, Y.; Shen, Q.; Li, J. Y.; Hu, L. H.; Li, J. *Biochim. Biophys. Acta.* **2006**, *1760*, 1505.
17. Zhang, Y. N.; Zhang, W.; Hong, D.; Shi, L.; Shen, Q.; Li, J. Y.; Li, J.; Hu, L. H. *Bioorg. Med. Chem.* **2008**, *15*, 8697.
18. Ottanà, R.; Maccari, R.; Amuso, S.; Wolber, G.; Schuster, D.; Herdinger, S.; Manao, G.; Camici, G.; Paoli, P. *Eur. J. Med. Chem.* **2012**, *50*, 332.
19. Liu, G.; Xin, Z.; Pei, Z.; Hajduk, P. J.; Abad-Zapatero, C.; Hutchins, C. W.; Zhao, H.; Lubben, T. H.; Ballaron, S. J.; Haasch, D. L.; Kaszubska, W.; Rondinone, C. M.; Trevillyan, J. M.; Jirousek, M. R. *J. Med. Chem.* **2003**, *46*, 4232.
20. Basu, S.; Prasad, U. V.; Barawkar, D. A.; De, S.; Palle, V. P.; Menon, S.; Patel, M.; Thorat, S.; Singh, U. P.; Das Sarma, K.; Waman, Y.; Niranjana, S.; Pathade, V.; Gaur, A.; Reddy, S.; Ansari, S. *Bioorg. Med. Chem. Lett.* **2012**, *22*, 2843.
21. Maccari, R.; Paoli, P.; Ottanà, R.; Jacomelli, M.; Ciurleo, R.; Manao, G.; Steindl, T.; Langer, T.; Vigorita, M. G.; Camici, G. *Bioorg. Med. Chem.* **2007**, *15*, 5137.
22. Ottanà, R.; Maccari, R.; Ciurleo, R.; Paoli, P.; Jacomelli, M.; Manao, G.; Camici, G.; Laggner, C.; Langer, T. *Bioorg. Med. Chem.* **2009**, *17*, 1928.
23. Guo, M.; Zheng, C. J.; Song, M. X.; Wu, Y.; Sun, L. P.; Li, Y. J.; Liu, Y.; Piao, H. R. *Bioorg. Med. Chem. Lett.* **2013**, *23*, 4358.
24. Jin, X.; Zheng, C. J.; Song, M. X.; Wu, Y.; Sun, L. P.; Li, Y. J.; Yu, L. J.; Piao, H. R. *Eur. J. Med. Chem.* **2012**, *56*, 203.
25. Xu, L. L.; Zheng, C. J.; Sun, L. P.; Miao, J.; Piao, H. R. *Eur. J. Med. Chem.* **2012**, *48*, 174.
26. Zheng, C. J.; Xu, L. L.; Sun, L. P.; Miao, J.; Piao, H. R. *Eur. J. Med. Chem.* **2012**, *58*, 112.
27. Shi, L.; Yu, H. P.; Zhou, Y. Y.; Du, J. Q.; Shen, Q.; Li, J. Y.; Li, J. *Acta Pharmacol. Sin.* **2008**, *2*, 278.
28. McGovern, S. L.; Helfand, B. T.; Feng, B.; Shoichet, B. K. *J. Med. Chem.* **2003**, *46*, 4265.
29. Molecular Operating Environment (MOE), **2014**; Chemical Computing Group Inc.: 1010

Sherbooke St. West, Suite #910, Montreal, QC, Canada, H3A2R7, 2014.09.

30. The 2D structures of the molecules were drawn in ChemBioDraw 2014 and converted to 3D in MOE v2014.0901 through energy minimization. The protonation state of the enzyme and the orientation of the hydrogens were optimized by LigX at pH 7 and a temperature of 300 K. Prior to docking, the force field of AMBER12: EHT and the implicit solvation model of Reaction Field (R-field) were selected. The docking workflow followed the “induced fit” protocol, in which the side chains of the receptor pocket were allowed to move according to the ligand conformations with a constraint on their positions. The weight used for tethering side chain atoms to their original positions was 10. All docked poses of molecules were ranked by London dG scoring first, and then a force field refinement was carried out on the top 30 poses followed by a rescoring using the GBVI/WSA dG scoring function.
31. Ajmani, S.; Karanam, S.; Kulkarni, S. A. *Chem. Biol. Drug Des.* **2009**, *74*, 582.

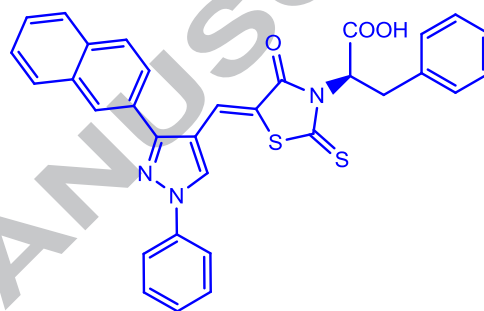
**Discovery of 1,3-diphenyl-1*H*-pyrazole derivatives containing
rhodanine-3-alkanoic acid groups as potential PTP1B inhibitors**

Liangpeng Sun^{a,1}, Peipei Wang^{b,1}, Lili Xu^c, Lixin Gao^b, Jia Li^{b,*}, Huri Piao^{c,*}



IIIv IC_{50} (PTP1B) = $0.67 \pm 0.09 \mu\text{M}$

IC_{50} (TCPTP) = $5.77 \pm 0.35 \mu\text{M}$



IVg IC_{50} (PTP1B) = $1.81 \pm 0.22 \mu\text{M}$

Two series of the 1,3-diphenyl-1*H*-pyrazole derivatives containing rhodanine-3-alkanoic acid groups were identified as competitive protein tyrosine phosphatase 1B (PTP1B) inhibitors.

Highlights

- Rhodanine-3-alkanoic acid groups were identified as pTyr mimetics.
- The most potent compound **IIIv** showed an IC₅₀ value of 0.67 ± 0.09 μM against PTP1B.
- The compound **IIIv** showed the best selectivity (9-fold) between PTP1B and TCPTP.
- Molecular docking studies supported the experimental observations.